High-purity H_2 production with CO_2 capture based on coal gasification

Kristin Jordal [a*], Rahul Anantharaman[a], Thijs A. Peters[b], David Berstad[a], John Morud[c], Petter Nekså[a] and Rune Bredesen[b]

[a] SINTEF Energy research, NO-7465 Trondheim, Norway
[b] SINTEF Materials and Chemistry, P.O. Box 124 Blindern, NO-0314 Oslo, Norway
[c] SINTEF Materials and Chemistry, R. Birkelands vei 2B, NO-7465 Trondheim, Norway

*Corresponding author: Phone: +47 416 47 397; fax: +47 735 97 250; e-mail: kristin.jordal@sintef.no

Abstract

A novel hybrid concept is proposed, combining Pd-alloy membrane and low temperature separation technology, to produce pure H_2 from gasified coal and capture the main part of the generated CO_2. 75% of the H_2 produced from gasification and water-gas shift is separated from the shifted syngas through H_2-selective Pd-alloy membranes. After water removal, the H_2-depleted, CO_2-rich retentate stream is compressed and cooled, after which CO_2 is condensed out at a purity level of ~99%. The "waste" volatiles from the low-temperature CO_2 separation constitute a low heating value syngas that is burnt in a gas turbine. The gas turbine with a steam bottoming cycle generates a surplus of electricity that could be employed for H_2 liquefaction. Altogether, the concept has the potential to be developed into a stand-alone high-purity H_2 production unit with CO_2 capture, suitable *e.g.* for remote areas from where H_2 and possibly also CO_2 must be transported by ship. However, the investigations of three different process alternatives, as well as three membrane separator parameters, illustrate that there are many degrees of freedom in the proposed concept that require further analysis, both individually and how they interact, in order to establish an optimized and purposeful stand-alone H_2 production concept.

Keywords

H_2 production; low-temperature CO_2 capture; coal gasification; H_2 liquefaction; Pd-alloy membranes

Abbreviations

HRF	Hydrogen Recovery Factor
HTS	High Temperature Shift
IGCC	Integrated Gasification Combined Cycle
IRCC	Integrated Reforming Combined Cycle
LH_2	Liquid Hydrogen
LHV	Lower Heating Value
LTS	Low Temperature Shift
PSA	Pressure-Swing Adsorption
WGS	Water-Gas Shift

1. Introduction

It is stated by the International Energy Agency (IEA) that in the long term, "completely eliminating fossil fuels in transport and industry without resorting to hydrogen may be hard to achieve" [1]. In the IEA *2°C scenario (2DS) – High H_2* in the same reference, a significant increase in the use of H_2 is projected, from current annual use of 6 EJ to nearly 30 EJ in 2050. With the abundant resources of fossil fuel in the world and the relatively low (but increasing) share of renewables in the energy mix, it is likely that a part of such an increase in H_2 use will rely on H_2 production from fossil fuels, including coal. In order to mitigate global warming, CO_2 capture must thus be applied in the H_2 production process. Consequently, H_2 production from fossil fuels, with Carbon Capture and Storage (CCS) may prove to be a key transition technology when moving in the direction of the hydrogen-based society.

In pre-combustion CO_2 capture power generation, the production of a H_2-rich gas turbine fuel is an intermediate step. For coal-based power production, the process under consideration is the Integrated Gasification Combined cycle (IGCC), whereas for natural gas, the process is called the Integrated Reforming Combined Cycle (IRCC). In both cases, the most mature CO_2 capture technology is to remove CO_2 from a shifted syngas using a solvent. Thereafter, the remaining gas turbine fuel contains, in addition to H_2, fractions of CO_2, CO, CH_4, and H_2O. In the case of IGCC, the fuel also contains N_2 and Ar, since nitrogen-rich waste gas from the cryogenic air separation unit is used for feeding of coal to the gasifier [2]. Compared to the challenge of handling the combustion of H_2 itself, the presence of these impurities in the gas turbine fuel does not constitute a problem for the combustor. However, there will be some CO_2 emissions from pre-combustion power plants.

In the case of co-production of power and H_2, or in the case of just producing H_2 from coal or natural gas for other use than gas turbine combustion (*e.g.* fuel cells or H_2 liquefaction for long-distance transport), CO_2 removal with solvents will not provide a sufficiently high H_2 purity. For industrial hydrogen, that requires a purity of 99.999%, a final purification of the hydrogen is usually achieved by pressure swing adsorption (PSA). For fuel cell applications, a preferential oxidation or selective methanation process is additionally required to reduce the CO content to a few ppm. An emerging separation technology that can be an alternative to these processes is the use of H_2-selective dense metal membranes. These membranes, based on palladium and its alloys, have frequently been proposed over the past decade to separate H_2 from a shifted syngas and simultaneously facilitate the capture of CO_2. An early outline of possible applications is given in [3]. In parallel with theoretical studies, this membrane technology has had a tremendous development and is now perceived as ready for scale-up and demonstration [4][5]. Power production with integrated Pd-alloy membrane reactors were evaluated and benchmarked in EU FP6 project CACHET [8]. In the subsequent EU FP7 project CACHET-II, integration of Pd-alloy membranes into power processes was

studied for the membrane water gas shift (M-WGS) process [8]-[14]. For IGCC applications, focus in [12] is put on the fact that the CO_2-rich stream leaving the membrane unit has a high concentration of impurities, due to the use of nitrogen for fuel feed to the gasifier, and what is referred to as "cryogenic purification" or "cryogenic separation" is employed for the retentate treatment, in order to reach sufficient CO_2 purity. The cryogenic process has a CO_2 capture rate ranging from 90 to 95%, depending on the CO_2 purity at the process inlet. In [14] a parametric investigation was made of "cryogenic methods" (flash tanks and distillation columns) for CO_2 separation in an IRCC process using Pd-alloy membranes for H_2 separation. A similar alternative for CO_2 separation, using flash tanks, and referred to as "low-temperature separation" has been developed independently at SINTEF [15][16]. The denomination "low-temperature" has been chosen here since the IRR International Dictionary [17] defines cryogenic as temperatures below 120 K or approximately -153°C. The fraction of membrane H_2 feed permeates through the Pd-alloy membrane, i.e. the hydrogen recovery factor (HRF), is varied from 76 to 98% in [12], and from 90-98% in [13], and the obtained very pure hydrogen is employed as gas turbine fuel. However, H_2 with such high purity can be more relevant to employ for other purposes than as gas turbine fuel in an IGCC or IRCC. Altogether:

- The retentate after Pd-alloy membrane separation of H_2 will always contain some combustible gases
- The most thermodynamically most efficient way to use a gaseous fuel for power production is in a gas turbine with a steam bottoming cycle
- The high CO_2 concentration in the retentate makes low-temperature separation a suitable capture technology. This technology requires power to run the external refrigeration cycle.
- High-purity hydrogen, as obtained with Pd-alloy membranes may be a suitable production method for H_2 that needs to be liquefied prior to transport. H_2 liquefaction requires power.

Hence, the hypothesis investigated in this paper is that it may prove to make sense not to maximize the HRF from a Pd-alloy separation process, but rather to match the H_2 production rate against the power generation required for CO_2 capture and potentially also H_2 liquefaction. More specifically, this paper performs a first evaluation of a novel hybrid concept for providing high purity H_2, to evaluate its potential to be developed into a self-sustained H_2 production process with CO_2 capture. Co-production of H_2 and electricity from coal with CO_2 capture has been suggested before, using Selexol and PSA [19], but not including the H_2 liquefaction perspective for stand-alone H_2 production units.

2. H_2 separation using Pd-alloy membranes

Pd-alloys have high solubility (*S*) and diffusivity (*D*) of H_2, and show great promise as membranes for medium to high temperature (> ~300 - 500°C) H_2 separation from shifted syngas, since they have a good temperature match with the operating conditions of the WGS reaction. Additionally, this type of membranes provides the best selectivity-flux combination of all the membrane classes [20]. The drawback

with Pd-alloy membranes is, however, that they are to various degrees prone to reduced H_2 permeation rates (poisoning) by the presence of strongly adsorbing species such as CO and sulphur, that block the H_2 dissociation sites [22]-[29], or even to complete deterioration of the membrane as in case of sulphur [30]-[32]. Sulphur removal after coal gasification is therefore critical for utilizing the full potential of Pd-alloy based membrane technology.

The H_2 flux through Pd-alloy membranes, F, ($mol \cdot m^{-2} \cdot s^{-1}$) is described by

$$F_{H_2} = \frac{SD}{L}\left[\left(P_{H_2}^{f}\right)^{n} - \left(P_{H_2}^{p}\right)^{n}\right] = \frac{Q}{L}\left[\left(P_{H_2}^{f}\right)^{n} - \left(P_{H_2}^{p}\right)^{n}\right] \quad (1)$$

where L is the membrane thickness, and $P_{H_2}^{f}$ and $P_{H_2}^{p}$ are the H_2 pressure on the feed and permeate side, respectively. The product of the diffusivity, D, ($m^2 \cdot s^{-1}$) and solubility, S, ($mol \cdot m^{-3} \cdot Pa^{-n}$) is often referred to as the H_2 permeability, Q. When the H_2 flux is limited by diffusion through the membrane material, the H_2 pressure exponent, n, is ideally equal to 0.5 (*i.e.* follows Sieverts' law). Variations in H_2 diffusivity and solubility with pressure, or surface contaminants, however, can alter the *n*-value. For example, an *n*-value close to 1 is typical for a membrane where the H_2 flux is governed by surface rate limitations. An experimentally obtained, realistic value for *n* is 0.63 [21].

As separation through the membrane occurs, a H_2-depleted layer is built up on the feed side, reducing the efficient partial pressure of H_2 at the membrane surface, and thereby also the gradient in H_2 partial pressure that sustains the flux through the membrane [22]. This effect is usually referred to as *concentration polarisation*.

Compared to the theoretical maximum performance of a H_2-separating Pd-alloy membrane, the relative contribution of concentration polarization and membrane poisoning mentioned earlier to reduced membrane performance depends on several parameters. Important parameters are membrane thickness, support material and porosity, operating temperature, pressure and feed gas composition. The performance of the membrane related to all these parameters should be determined in experimental testing. For example, for highly permeable 1-3 µm thick Pd-23at% H_2 selective membranes operated in inert gas mixtures, the H_2 flux is mainly limited by gas phase diffusion limitation at the feed side [22].

3. Membrane process unit for H_2 separation

In combination with the WGS process, the use of H_2-separating membranes can be investigated in two possible ways, either as a WGS-membrane reactor (WGS-MR) [6][7], or as a sequential arrangement of water-gas shift reactors and membrane separator modules [10]-[13]. The first alternative means that the H_2 membrane is envisaged to be integrated in the WGS reactor, for simultaneous H_2 production and removal, thus shifting the WGS reaction towards higher yield.

Figure 1.

In the CACHET-II project the alternative investigated was to apply separate modules of WGS reactors and membrane separators in series (refer to Figure 1). There are several advantages with this concept with regard to optimization of size, operation, feed flowrate and maintenance but there is also a potential downside in terms of increase in catalyst volume and membrane area combined to an integrated WGS-MR [33]. An application to gasified coal with the sequential concept shown in Figure 1 was investigated in [12][13] for the IGCC, and an extended analysis is provided in [34], where it is concluded that the expected number of WGS reactors in series according to the principle shown in Figure 1 will be three. An important difference between the IGCC case and the H_2 production concept presented in this paper is that a higher HRF is targeted for IGCC (typically 90%). It can also be noted that for the natural-gas based IRCC, a HRF of 90-95% is analysed, and that two WGS reactors in series appears to be the optimum configuration [35].

As mentioned in section 2, the thickness of the Pd-alloy membranes is in the order of a few microns. Hence, as indicated in Figure 1, the membrane is applied on a porous mechanical support. In order to reduce the partial pressure of the H_2 on the permeate side and increase the driving force over the membrane, one may apply an inert sweep gas (*e.g.* nitrogen) on the permeate side. This is especially relevant when the permeate side of the membrane is operated at elevated pressure. Alternatively, a high absolute pressure difference is required over the membrane. This may be achieved by maintaining a low vacuum on the permeate side [36].

When integrating the H_2 membrane in an IGCC, with the sole purpose of producing electric power, it is preferable from an efficiency point of view to maximize the HRF through the membrane units, although this is not necessarily the optimum from an economic point of view, due to increased membrane cost, as shown in [12]. However, in the present paper, maximising the HRF in itself is not a target. A certain amount of H_2 should on purpose remain in the retentate, in order to provide (a part of) the chemical energy required in the gas turbine fuel. Also, integrating the WGS reaction with the membrane separation would add complexity in the investigation of the hydrogen separating unit without increasing the knowledge about the overall hydrogen production concept. Hence, for this first concept study it was chosen to focus on a process alternative with only one membrane stage, applied downstream of the WGS reactor(s), and not a series of membrane stages separated by WGS reactors, although this may be a relevant alternative for future studies. Furthermore and importantly, the objective is to produce high-purity H_2, which means that it is not preferable to apply a sweep gas. Steam could indeed be envisaged as sweep gas, but this would require water condensation and drying in order to obtain high-purity H_2, which would further complicate the concept.

The tubular membrane applied in the membrane process unit have the configuration shown in

Figure *2*, where in practice an industrial membrane process unit will consist of a large number of tubular membrane modules connected in parallel. The diameter d_1 indicates how the diameter for the feed syngas

that surrounds one membrane is considered in the membrane separator computational model applied in the present work. The circular shape is an approximation, since the membranes typically would be arranged in a hexagonal pattern [37].

Figure 2.

4. H_2 production and CO_2 capture concept

4.1. Concept overview

The novel concept for production of high-purity H_2 with CO_2 capture from gasified coal proposed in this paper, is schematically illustrated in Figure 3. The concept uses, as far as possible, the Shell hard coal gasifier, syngas cooling and sulfur removal processes as described by the European Benchmarking Task Force (EBTF) [2]. Following the EBTF specifications, the gasifier is fed with oxygen of 95% purity and the syngas has an outlet pressure of 44 bar and an outlet temperature of 1550°C before the cleaning and cooling. After cleaning and cooling, the syngas is at 41 bar and 170°C and is sent to sulfur removal down to single-digit ppm level (using Selexol [2]). A modification done compared to the EBTF is that sulfur is removed upstream of the water-gas shift (WGS) – the level of H_2S in the membrane feed gas is critical for the performance and should preferentially be less than 2-3 ppm, depending on operating temperature and H_2 concentration. Thereafter, in *Case 1* of the concept, the CO/H_2-rich syngas is sent to a high-temperature water-gas shift (HTS) reactor only, with the outlet CO concentration set to 3%, which requires substantial amounts of steam in the HTS reactor. The reason for this case is that there is a good temperature match between the HTS reactor outlet and the Pd-membrane operating temperatures (400°C). However, as investigated in *Case 2*, adding a low-temperature water-gas shift (LTS) reactor reduces the amount of steam required, increases the H_2 concentration on the membrane feed side, and converts most of the CO to CO_2. This can increase the average H_2 flux through the membrane, and therefore with a maintained HRF, leads to a reduction in required membrane area, while also a higher CO_2 capture rate is possible to obtain. But it also means that heating of the shifted syngas is required before entering the membrane separator, which complicates the process heat integration slightly. In the present work, the syngas was heated to 400°C.

As can be seen in Equation 1, the H_2 partial pressure difference is the driving force for H_2 separation. Therefore, Case 3 was investigated with HTS and LTS reactors as for Case 2, but with a syngas compressor upstream of the shift reactors. The feed pressure of the shifted syngas to the membrane separator is therewith increased from 41 to 60 bar. It is recognized by the authors that a total pressure difference of 59 bar over the membrane + porous support may pose practical challenges.

4.1.1. Simulating membrane separation of H_2

The first target with the evaluation of this novel process concept has been to close the heat and mass balance. After initial evaluations it was decided to undertake this first concept study with a HRF of 75% for all three cases, since this appeared to be close to the HRF for a self-sustained process. It is beyond the scope of this first study to optimize the process and find the HRF that matches a self-sustained process exactly. The membrane separator simulation with a HRF of 75% was performed with a spreadsheet-based simulation tool developed by SINTEF for membrane separator and membrane reactor simulations in the CACHET-II project [37]. The tool has previously been employed in *e.g.* [11][13][18], and integrates a mass transfer model through the membrane using a corrected Sieverts law with a mass transfer through the support calculated using a Dusty Gas model. In addition, the model takes external mass transfer limitations in the gas-phase into account using engineering correlations.

Figure 3.

The input assumptions and total membrane area for the membrane separation simulations can be seen in Table ***1***. The total inlet molar flow of shifted syngas is determined by the size of the Shell-type gasifier in the EBTF [2]. A molar flow of 1 mol/s per tubular membrane was used in the simulations. The membrane length L_T was adjusted to obtain a HRF of 75%. Membrane permeation data represents current performance of state-of-the art Pd-alloy membranes.

Table 1.

4.1.2. Low-temperature CO_2 separation

After separation of H_2 through the membrane, the remaining CO_2-rich retentate stream is cooled and dried, first through water condensation, thereafter with adsorptive dehydration such as molecular sieves or similar, in order to avoid freeze-out and clogging of heat exchangers in the low-temperature CO_2 separation process. Thereafter it is sent to a low-temperature separation process. In this unit [15][16], the syngas is compressed and subsequently cooled down to temperatures approaching -56°C. The required compression work will depend on the retentate pressure and required separator pressure. The main part of the CO_2 condenses and can thus be separated through phase separation at purity levels around or exceeding 99%. One possible layout for the low-temperature separation process is shown in Figure 4. It can be observed that the volatiles from the separation process, indicated as GT fuel, are expanded and heated after the separation process in order to recover energy and thus to improve the separation process efficiency. After the second phase separator, CO_2 is in the liquid state at 7–10 bar which is directly compatible with ship transport of CO_2. For pipeline transport the liquid CO_2 is, as illustrated in Figure 4, heated and pumped to 110 bar.

Figure 4.

4.1.3. Stream compositions before and after separation processes

Composition of streams before and after the syngas separation processes are given for Cases 1-2 in Table 2 and *Table 3*. (The stream data for Case 3 deviate from Case 2 with less than 0.3% and are therefore not provided here.) The low-temperature capture process parameters were adjusted so that 90% of the CO_2 that enters that process is liquefied and captured. In Case 1, the resulting low heating value syngas (stream 5 in table 2, GT fuel at 20 bar in Figure 4) contains ~16% CO, which will reduce the overall CO_2 capture rate. The CO concentration is reduced in stream 5 for (Cases 2 and 3), meaning that the CO_2 capture rate is improved. Cases 2 and 3 also will have an increased overall H_2 yield.

Table 2.

Table 3.

4.1.4. Gas turbine model

The syngas GT fuel is delivered from the low-temperature capture process at 20 bar and 74.1°C with a Lower Heating Value (LHV) of 8.75 MJ/kg for Case 1 and 9.49 MJ/kg for Cases 2 and 3. This means that the heating value of this gas is well within the range of what can be burnt in existing gas turbines designed for low-grade fuels.

In order to simulate combustion of the syngas GT fuel in a gas turbine, a gas turbine model was set up in Aspen HYSYS, to reflect open data for the SGT5-2000E. This gas turbine model was formerly sold under the name of Siemens V94.2, which is the gas turbine model that was employed in the Buggenum IGCC plant. After obtaining a good match with open data for the SGT5-2000E for a natural gas fuel simulation, the model was applied to syngas fuel combustion. The compressor pressure ratio was then increased with 5%, to accommodate for some of the increased volume flow in the gas turbine. The size of the gas turbine simulated in the present work in terms of power output is approximately 50% of a SGT5-2000E. It is not claimed that the performance of the gas turbine model in the present work mirrors the performance of the SGT5-2000E perfectly, although the gas turbine model in this paper should have an efficiency (~34.4% on natural gas in stand-alone operation) that reflects the technology level of gas turbine capable of burning a low heating value fuel.

4.1.5. Steam generation and steam bottoming cycle

The gas turbine exhaust heat can be employed to generate steam required for the WGS reactor(s), and for the regeneration of Selexol applied for H_2S removal. There is also enough heat available in the exhaust to

generate HP and LP steam in a steam bottoming cycle. Additional IP steam to the steam bottoming cycle is provided from the gasifier island, where steam generation is the means to cool the hot syngas after gasification. Heat is also recovered into the steam cycle as the H_2-depleted syngas and H_2 product stream is cooled after the membrane process unit. Altogether, the heat integration of the investigated process is rather complex, and was achieved using Pinch Analysis. The composite curves of all hot and cold streams for the case 1 hydrogen production process (i.e. with HTS only) is shown in

Figure *5*. It is noteworthy that a standard Gas Turbine Combined Cycle is not applicable; the steam cycle needs to be tailored for this application.

Figure 5.

4.2 – Results from heat and mass balance calculations

Aspen HYSYS process simulations were used to determine the overall heat and mass balance for Cases 1, 2 and 3. The results from the heat and mass balance simulations are given in Table 4.

It can be seen that for the assumed hydrogen recovery factor of 75%, without any further processing of the hydrogen, the heat and mass balances are closed with a small excess power production, ~18% for Case 1 and 16% for Cases 2 and 3. Case 1 produces less hydrogen than Cases 2 and 3 since it only has the HTS reactor, but the overall first law efficiency (adding upp electric power and H_2 chemical energy) is in the same range for all cases, 63.5-65.1%. Increasing the HRF would have decreased or eliminated the surplus power, but referring back to section 4.1.1, it has not been the target of the present concept study to match the HRF exactly with a self-sustained process. It can be observed, as was already indicated when comparing Tables 2 and 3, that the CO_2 capture rate increases from Case 1 79.9%) to Cases 2 and 3 (89.7%). The results in Table 4 provide some insight to the concept illustrated in Figure 3, and also show the differences between two different hydrogen production rates: The hydrogen recovery rate is 75% in both cases, but due to a higher CO conversion in Cases 2 and 3, these cases produce more H_2 (2.15 kmole/s = 4.33 kg/s) than Case 1 (2.01 kmole/s =4.06 kg/s). If one should target to obtain the same hydrogen production rate with Cases 2 and 3 as is obtained with Case 1, the HRF could be reduced to 70.2%, which would also increase the electric power production. When comparing Cases 2 and 3, it can be seen that the membrane area decreases (as expected) when the partial pressure difference increases over the membrane.

Table 4.

5 – Process performance with H_2 liquefaction

The excess power provided by the concepts investigated in this paper, together with the high purity H_2 that can be obtained through Pd-alloy membrane separation is a good starting point for H_2 liquefaction; the H_2 that is available at 1 bar and 400°C will first have to be cooled before it can be compressed and liquefied. H_2 liquefaction has been studied recently in the EU FCH-JU research project IDEALHY [38]. Current state-of-the-art technology for H_2 liquefaction lies around 12 kWh/kg LH_2 produced (boundary conditions 20 bar and 30°C). IDEALHY concluded that more advanced H_2 liquefaction technologies for the mid- to long-term development would require 6.40 kWh_e/kg LH_2 [39][40]. In addition, the specific work required for compressing H_2 cooled to 30°C from 1 bar a to 20 bar a can be calculated to 1.7 kWh/kg H_2. The power consumption and power deficit/power surplus for liquefaction applied to the H_2 produced with Cases 1 and 2 can be seen in *Table 5*.

Table 5.

The final energy efficient process design in IDEALHY was for a LH_2 plant of 50 metric tonnes/ day, whereas 4.06 kg/s H_2 corresponds to ~350 metric tonnes per day. In order to produce such quantities, several parallel LH_2 modules would have to be installed. It should be noted in this context that he largest existing LH_2 plants today are capable of producing around 10 tonnes of LH_2/day [42].

Hence, with conventional technology, even when taking into account the additional power generated from heat recovered through H_2 cooling, there is an electric power deficit of ~75 MW_e for Case 1 and due to the increased H_2 conversion with maintained HRF this deficit increases to ~107 MW_e for Case 2. Hence, with current liquefaction technology, a HRF of ~75% is far too elevated for a self-sustained H_2 production and liquefaction plant. For advanced H_2 liquefaction technology, there is an excess power production of ~6 MW_e, for Case 1 and a power deficit of 20 MW_e for Case 2, which is rather close to a self-sustained H_2 production process.

When producing liquid hydrogen, less than 1 ppm of trace impurities (N_2, O_2, Ar, etc.) can be tolerated [41]. For conventional hydrogen production plants (PSA technology), the impurities fraction of produced H_2 is typically around 10 ppm, and a final H_2 purification step must then be introduced with regenerative low-temperature adsorption at around 80 K [41]. Pd-alloy membranes are selective to H_2 only, and provided that no unselective transport occurs, a low-temperature hydrogen purification unit does not have to be active or not even included for normal operation mode of a hydrogen liquefaction process.

6. Investigation of membrane separator behaviour

It is clear from the above concept study that the heat and mass balance can be closed, and that a HRF of around 70-75% could be a suitable target for a self-sustained process with CO_2 capture when using future

H_2 liquefaction technology. There are however a tremendous amount of variables for the overall process as well as for the membrane separator that require further investigation. For the overall process, this has been illustrated through Cases 1-3, and for the membrane separator it is illustrated in this section by varying three variables for Cases 1 and 2: the tubular membrane length, the permeate pressure and the membrane thickness.

Figure 6.

There are practical limitations on tubular membrane length form a manufacturing point of view, and, due to the absence of sweep gas, the lengths obtained in the present study when HRF is set to 75% are significant and may pose a challenge. The current limitation mainly lies in the available length of the porous support. It can be seen in Figure 6 how the HRF decreases with decreasing membrane length. It can also be seen that, because the H_2 concentration is higher on the feed side in Case 2, shorter membrane tubes are required. Reducing the HRF to ~70% in Case 2, as mentioned above, would further decrease the tube length and membrane area.

It is evident from the results shown in Figure 7 that it is paramount for the realization of a HRF of 75% that the membrane unit operates with a high absolute pressure difference, but it can also be seen that because the H_2 concentration is higher on the feed side in Case 2, the sensitivity with respect to permeate pressure is slightly reduced. From an overall process design point of view it should be preferable if the permeate side pressure can be increased, since this decreases the compression power required for hydrogen liquefaction, and an alternative for reducing HRF to 70% as mentioned above would correspond to increasing the permeate pressure to ~2 bar. However, for a more significant permeate pressure increase, the feed side pressure must be increased at the same time to obtain sufficient driving force for H_2 permeation (refer to Eq. 1). Altogehter, the membrane separator performance and required HRF would have to be analysed together with the compression power requirements upstream of the WGS reactors in combination with the compressors for the low-temperature CO_2 separation and H_2 liquefaction - a complex but highly relevant task for future investigations.

Figure 7.

Intuitively, when studying equation 1, it could be expected that a measure to counteract the high absolute pressure difference requirement for H_2 recovery would be to reduce membrane thickness. However, within the range that is relevant for current and anticipated future membrane technology, the impact of varying the membrane thickness is rather negligible for the applied H_2 separation module configuration, as can be seen in Figure 8.

Figure 8.

An explanation is that under the investigated membrane operating conditions, the H_2 flux through the membrane is limited by concentration polarization (refer to section 2). A decrease in membrane thickness will therefore not affect the HRF significantly. The effect of concentration polarization may be reduced through a decrease in the difference between d_1 and d_2 (refer to

Table ***1***), however, this is at the expense of an increased feed side pressure drop, and therefore an optimization must be performed. Alternatively, these gas phase limitations can be reduced by smart module design in order to optimize feed flow conditions to reduce the thickness of the hydrogen-depleted layer. Microstructured membrane reactors that reduce gas phase diffusion limitations and increase the membrane area to reactor volume ratio compared to traditional tubular reactors, offer in this respect great advantages [43].

7. Conclusions and future work

This paper presents a novel hybrid concept for production of high-purity H_2 from gasified coal, with CO_2 capture. The concept features separation of H_2 through H_2-selective Pd-alloy membranes, followed by low-temperature capture of CO_2. The remaining gas mixture has a low heating value (~8.8-9.5 MJ/kg), and can be used as gas turbine fuel with existing technology. Three cases were investigated where 75% of the produced H_2 is recovered through the membrane. Due to the presence of CO in the gas turbine fuel, the overall CO_2 capture rate is 80% for a case with HTS only, and 90% with HTS + LTS, regardless of permeate feed pressure. The net power generated in the process is approximately sufficient for liquefying the separated H_2 (HRF 75%), with advanced future liquefaction technology.

Altogether it can be concluded that many pieces must match to make the suggested concept a viable H_2 production technology with CO_2 capture. For a self-sustained process employing advanced liquefaction technology it appears that the HRF should be 70-75%.

The many degrees of freedom in the concept that deserve to be further analysed, both individually and how they interact open up for further process optimisation. It is clear from the undertaken study that CO conversion should be maximized to reduce CO_2 emissions and membrane area, but the interplay between HRF and e.g. membrane length and permeate pressure needs further investigations. It should also be of interest to investigate the reduction of concentration polarization effects and how this would affect membrane sizing and module design. Increasing the pressure levels on both feed and permeate sides of the membrane separation unit is relevant to investigate, in order to reduce power requirements for H_2 liquefaction and CO_2 capture.

The H_2 liquefaction process was not integrated with the low-temperature CO_2 capture process in this study. The liquefaction of CO_2 and hydrogen requires cooling to temperature levels around -60°C and -250°C, respectively, requiring different refrigerants and cycle configurations, cold-box insulation standards and

other equipment standards in order to function optimally. Attempting to establish a common integrated low-temperature/cryogenic process is not feasible from the viewpoint of process practicalities nor from efficiency perspectives. The cycle layouts have high degree of internal heat recuperation and do not have additional cooling available for each other.

Acknowledgments

This publication has been produced with support from the BIGCCS Centre, performed under the Norwegian research program *Centres for Environment-friendly Energy Research (FME)*. The authors acknowledge the following partners for their contributions: Gassco, Shell, Statoil, TOTAL, GDF SUEZ and the Research Council of Norway (193816/S60).

References

[1] IEA. Energy Technology Perspectives 2012.

[2] Franco, F., Anantharaman, R., Bolland, O., Booth, N., van Dorst, E., Ekstrom, C., Fernandes, E.S., Macchi, E., Manzolini, G., Nicolic, D., Pfeffer, A., Prins, M., Rezvani, S., Robinson, L., 2011. "Test cases and preliminary benchmarking results from the three projects", http://caesar.ecn.nl/fileadmin/caesar/user/documents/D_4.9_best_practice_guide.pdf

[3] Bredesen, R., Jordal, K., Bolland, O. High-temperature membranes in power generation with CO_2 capture. Chemical Engineering and Processing 43 (2004), 1129-1158.

[4] Carbon Sequestration Leadership Forum. October 2013. Final Report by the CSLF Task Force on CCS Technology Opportunities and Gaps.

[5] Veenstra, P., Iyer, M., Nijmeijer, A., Geuzebroek, F., Moene, R., Saukaitis, J. Integrated Approach to CO_2 Capture: fuel gas decarbonisation. Energy Procedia, 63 (2014) 2054-2059.

[6] Basile, A., Chiappetta, G., Tosti, S., Violante, V. Experimental and simulation of both Pd and Pd/Ag for a water gas shift membrane reactor, Separation and Purification Technology, 2001, 25, 549-571.

[7] Tong, J.H., Matsumura, Y., Suda, H., Haraya, K. Experimental study of steam reforming of methane in a thin (6 mu M) Pd-based membrane reactor, Industrial & Engineering Chemistry Research, 2005, 44, 1454-1465

[8] Beavis, R. The EU FP6 CACHET project - Final results, Energy Procedia, 2011a, 4, 1074-1081.

[9] Beavis, R., CACHET-II: Carbon capture and hydrogen production with membranes–A new in project in FP7-Energy. Energy Procedia, 2011b, 4, 745-749. doi:10.1016/j.egypro.2011.01.114

[10] Atsonios, K, Panopoulos, K.D., Doukelis, A., Koumanakos, A., Kakaras, Em. (2012) Exergy analysis of a hydrogen fired combined cycle with natural gas reforming and membrane assisted shift reactors for CO_2 capture. Energy Conversion and Management 60, 196-203.

[11] Atsonios, K, Panopoulos, K.D., Doukelis, A., Koumanakos, A., Morud, J., Kakaras, Em. (2013) Natural gas upgrading through hydrogen selective membranes: Application in Carbon Free Combined Cycles. Energy procedia 37, 914-923.

[12] Manzolini, G., Gazzani, M., Turi, D.M., Macchi, E. Application of hydrogen selective membranes to IGCC, Energy Procedia 37 (2013) 2274-2283.

[13] Gazzani, M., Turi, D.M., Manzolini, G. 2014. Techno-economic assessment of hydrogen selective membranes for CO_2 capture in integrated gasification combined cycle. International Journal of Greenhouse gas Control 20 (2014) 293-309.

[14] Atsonios, K., Panopoulos, K.D. Doukelis, A. Koumanakos, A. Kakaras, E. Cryogenic method for H_2 and CH_4 recovery from a rich CO_2 stream in pre-combustion carbon capture and storage schemes, Energy, 53 (2013) 106-113.

[15] Berstad, D., Anantharaman, R., Nekså, P., 2013a. Low-temperature CO_2 capture technologies – Applications and potential. International Journal of Refrigeration 36(5), 1403–1416.

[16] Berstad, D., Anantharaman, R., Nekså, P., 2013b, Low-temperature CCS from an IGCC power plant and comparison with physical solvents, Energy Procedia 37, 2204–2211.

[17] International Institute of Refrigeration. International Dictionary of Refrigeration. Peeters Publishers, Leuven (2007).

[18] Van Berkel, F., Hao, C., Bao, C., Jiang, C., Xu, H., Morud, J., Peters, T., Soutif, E., Dijkstra, J., Jansen, D., Song, B. Pd-membranes on their way towards application for CO_2-capture. Energy Procedia 37 (2013) 1076-1084. doi: 10.1016/j.egypro.2013.05.204

[19] Chiesa, P., Consonni, S., Kreuts, T., Williams, R. Co-production of hydrogen and CO_2 from coal with commercially ready technology. Part A: Performance and emissions. International Journal of Hydrogen Energy 30 (2005) 747-767. doi:10.1016/j.ijhydene.2004.08.002

[20] Ockwig, N.W., Nenoff, T.M. Membranes for hydrogen separation, Chemical Reviews, 2007, 107, 4078-4110.

[21] Peters, T.A., Stange, M., Bredesen, R. On the high pressure performance of thin supported Pd–23%Ag membranes—Evidence of ultrahigh hydrogen flux after air treatment. Journal of Membrane Science, 2011, 278, 28-34.

[22] Peters, T.A., Stange, M., Klette, H., Bredesen, R. High pressure performance of thin Pd-23%Ag/stainless steel composite membranes in water gas shift gas mixtures; influence of dilution, mass transfer and surface effects on the hydrogen flux, Journal of Membrane Science, 2008, 316, 119-127.

[23] Amandusson, H., Ekedahl, L.G., Dannetun, H. The effect of CO and O-2 on hydrogen permeation through a palladium membrane, Applied Surface Science, 2000, 153, 259-267

[24] Mejdell, A.L., Jøndahl, M., Peters, T.A., Bredesen, R., Venvik, H.J. Effects of CO and CO_2 on hydrogen permeation through a ~3um Pd/Ag 23wt.% membrane employed in a microchannel membrane configuration, Separation and Purification Technology, 2009, 68, 178-184.

[25] Nguyen, T.H., Mori, S., Suzuki, M. Hydrogen permeance and the effect of H2O and CO on the permeability of Pd0.75Ag0.25 membranes under gas-driven permeation and plasma-driven permeation, Chemical Engineering Journal, 2009, 155, 55-61

[26] Catalano, J., Giacinti Baschetti, M., Sarti, G.C. Hydrogen permeation in palladium-based membranes in the presence of carbon monoxide, Journal of Membrane Science, 2010, 362, 221-233

[27] Unemoto, A., Kaimai, A., Sato, K., Otake, T., Yashiro, K., Mizusaki, J., Kawada, T., Tsuneki, T., Shirasaki, Y., Yasuda, I. Surface reaction of hydrogen on a palladium alloy membrane under co-existence of H_2O, CO, CO_2 or CH_4, International Journal of Hydrogen Energy, 2007a, 32, 4023-4029

[28] Unemoto, A., Kaimai, A., Sato, K., Otake, T., Yashiro, K., Mizusaki, J., Kawada, T., Tsuneki, T., Shirasaki, Y., Yasuda, I. The effect of co-existing gases from the process of steam reforming reaction on hydrogen permeability of palladium alloy membrane at high temperatures, International Journal of Hydrogen Energy, 2007b, 32, 2881-2887

[29] Gallucci, F, Chiaravalloti, F. Tosti, S. Drioli, E. Basile, A. The effect of mixture gas on hydrogen permeation through a palladium membrane: Experimental study and theoretical approach, International Journal of Hydrogen Energy, 2007, 32, 1837-1845

[30] Chen, C.H., Ma, Y.H. The effect of H_2S on the performance of Pd and Pd/Au composite membrane, Journal of Membrane Science, 2010, 362, 535-544

[31] O'Brien, C.P., Howard, B.H., Miller, J.B. Morreale, B.D., Gellman, A.J. Inhibition of hydrogen transport through Pd and Pd47Cu53 membranes by H_2S at 350C, Journal of Membrane Science, 2010, 349, 380-384

[32] Mundschau, M.V., Xie, X. Evenson, C.R. Sammells, A.F. Dense inorganic membranes for production of hydrogen from methane and coal with carbon dioxide sequestration, Catalysis Today, 2006, 118, 12-23

[33] P.Middleton, P.Hurst, G.Walker, in D.C.Thomas (Ed.), Carbon dioxide capture for storage in deep geological formations - results from the CO2 capture project;capture and separation of carbon dioxide from ombustion sources, Elsevier,Naperville, 2005. Chapter 23 GRACE: Pre-Combustion De-Carbonisation Hydrogen Membrane Study

[34] Gazzani, M., Manzolini, G. Using palladium membranes for carbon capture in integrated gasification combined cycle (IGCC) power plants. In: Doukelis A, Panopoulos K, Koumanakos A and Kakaras E, (eds.). Palladium Membrane Technology for Hydrogen Production, Carbon Capture and Other Applications. Woodhead Publishing, 2015, p. 221-246.

[35] Atsonios, K., Koumanakos, A., Panopoulos, K.D., Doukelis, A., Kakaras., E. Using palladium membranes for carbon capture in natural gas combined cycle (NGCC) power plants: process integration and techno-economics. In: Doukelis A, Panopoulos K, Koumanakos A and Kakaras E, (eds.). Palladium Membrane Technology for Hydrogen Production, Carbon Capture and Other Applications. Woodhead Publishing, 2015, p. 247-85.

[36] Kurokawa, H., Shirasaki, Y., Yasuda, I. Energy-Efficient Distributed Carbon Capture in Hydrogen Production from Natural Gas. Energy Procedia 4(2011) 674-680.

[37] Morud, J.C. Simulation of palladium membrane reactors: a simulator developed in the CACHET-II project In: Doukelis A, Panopoulos K, Koumanakos A and Kakaras E, (eds.). Palladium Membrane Technology for Hydrogen Production, Carbon Capture and Other Applications. Woodhead Publishing, 2015, p. 193-211.

[38] Berstad, D., Börsch M., Decker, L., Elliott, A., Haberstroh, C., Louis, J., Lowesmith, B., Mortimer, N., Nekså, P., Quack, H., Seeman, I., Stolzenburg, K., Walnum, H.T., 2013c. IDEALHY – Integrated Design for Demonstration of Efficient Liquefaction of Hydrogen. Presented at Hydrogen & Fuel Cells in the Nordic Countries 2013, November 1st 2013, Oslo, Norway, http://www.hydrogen.no/Kalender/2013/HFCNordic_2013/presentations/c2/IDEALHY_HFCNordic2013.pdf [accessed 15.01.2014]

[39] Berstad, D., Nekså, P., Walnum, H.T., Decker, L., Elliott, A., Quack, H., 2013. IDEALHY – Report on Efficiency and Cost Calculations (Restricted report). Summary and Table of contents available from: http://www.idealhy.eu/uploads/documents/IDEALHY_D2-7_Efficiency_and_Cost_Summary_web.pdf

[40] Blum, L., Decker, L., Ohlig, K., 2013. IDEALHY – Industry Audit on Evaluated Process (Restricted report). Summary and Table of contents available from: http://www.idealhy.eu/uploads/documents/IDEALHY_D2-8_Report_on_Process%20Audit_Summary_web.pdf

[41] Bracha, M., Lorenz, G., Patzelt, A., Wanner, M. Large-scale hydrogen liquefaction in Germany. Int. J. Hydrogen Energy 1994, 19, 53-59.

[42] Krasae-in, S., Stang, J.H., Neksa, P. Development of large-scale hydrogen liquefaction processes from 1898 to 2009. International Journal of Hydrogen Energy 35 (2010) 4524-4533.

[43] Mejdell, A.L., Jøndal, M., Peters, T.A., Bredesen, R. Experimental investigation of a microchannel membrane configuration with a 1.4 µm Pd/Ag23 wt.% membrane-Effects of flow and pressure. Journal of Mermbrane Science 327(2009) 6-10. DOI: 10.1016/j.memsci.2008.11.028

Highlights

- A novel process concept for H_2 production with CO_2 capture is presented
- Pd-alloy membrane for high H_2 purity combined with low-temperature CO_2 capture
- Purity of both H_2 and CO_2 sufficient for ship transport
- Waste volatiles burnt in gas turbine for power generation
- The concept can be developed for stand-alone H_2 production with CO_2 capture

Figure 1

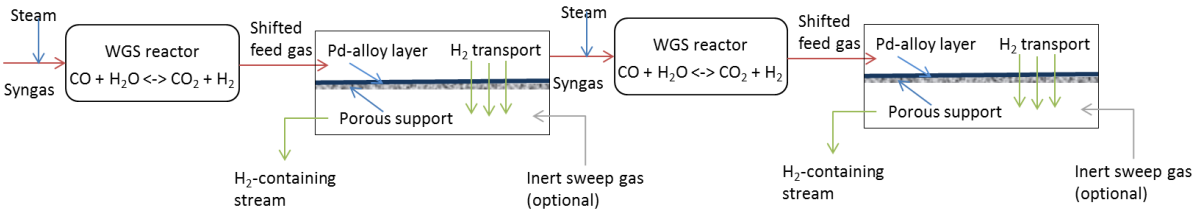

Figure 1. Principle of sequential H_2 production in WGS reactors and subsequent separation with Pd-alloy membranes.

2 column figure

Figure 2

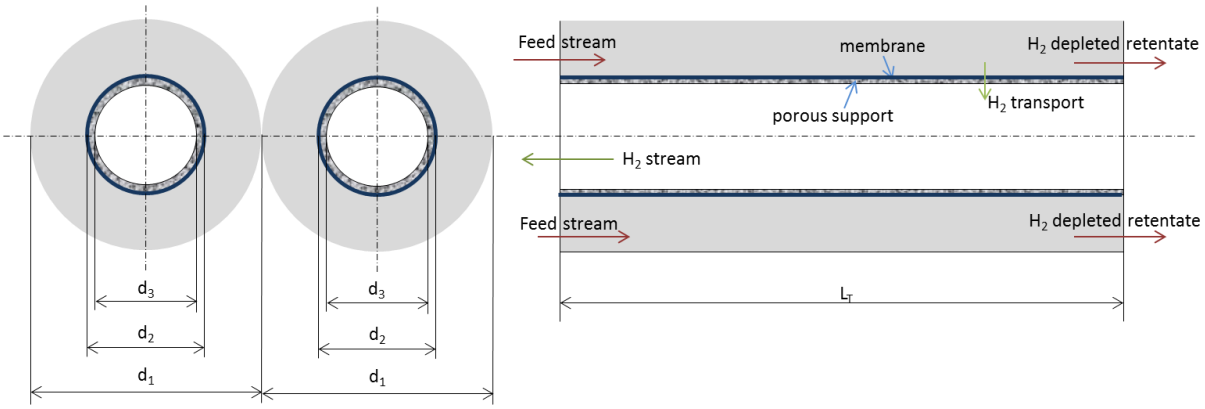

Figure 2. Principle of tubular membrane separator without sweep gas. The industrial process unit will consist of a large number of tubular membrane modules arranged in a hexagonal configuration.

2 column figure

Figure 3

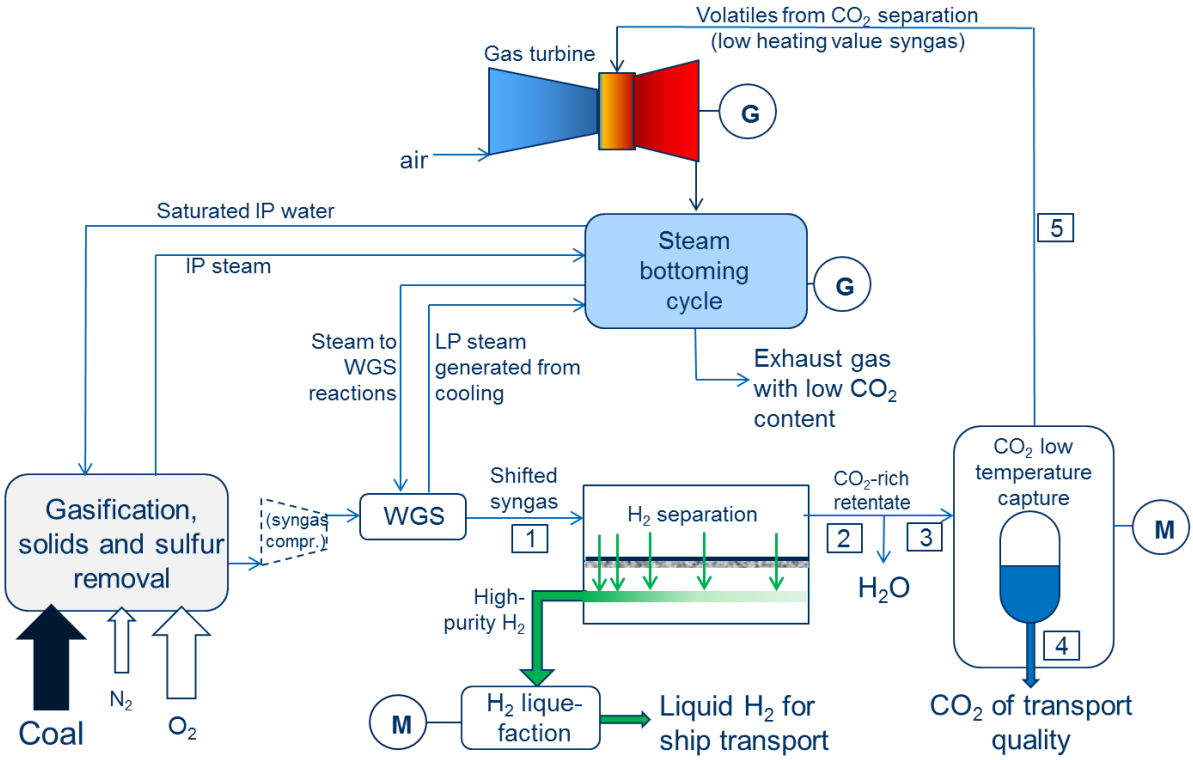

Figure 3. Proposed novel concept for H_2 production using H_2-separating membranes in combination with low-temperature CO_2 capture. Stream numbers refer to tables 2-4.

2 column figure

Figure 4

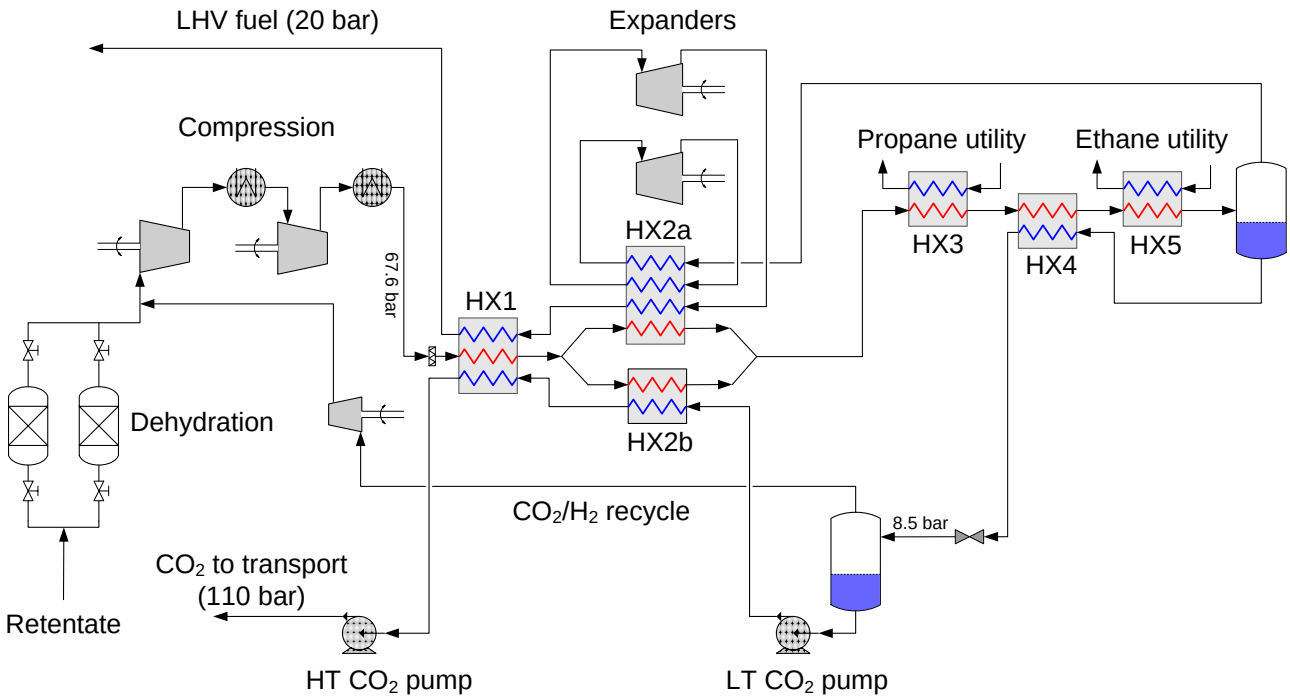

Figure 4. Process flow diagram for low-temperature separation of CO_2 from syngas.

1.5 column

Figure 5

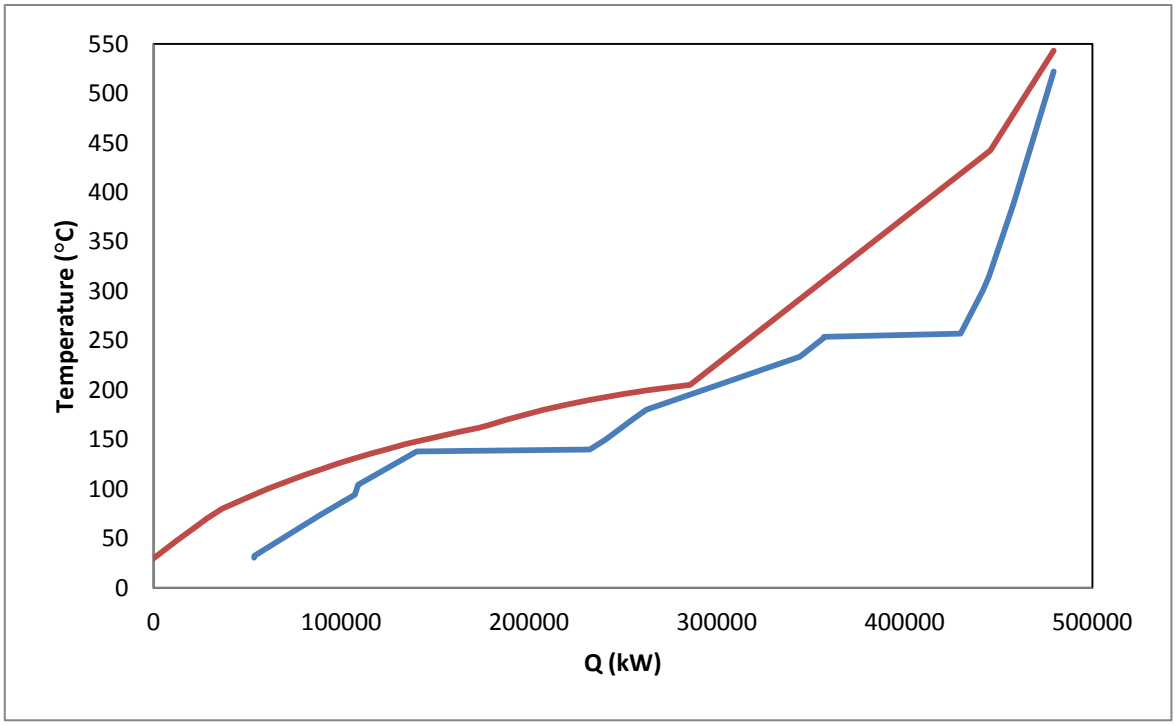

Figure 5. Composite curves for the integrated hydrogen production process.

Figure 6

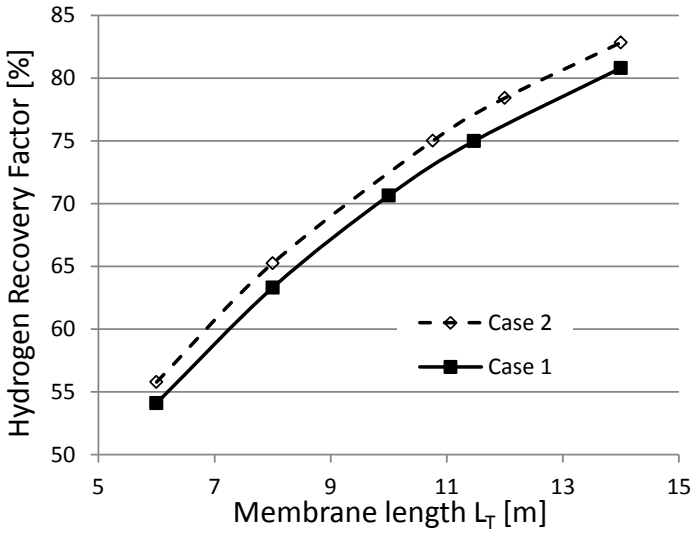

Figure 6. HRF dependency on membrane length.

1 column figure

Figure 7

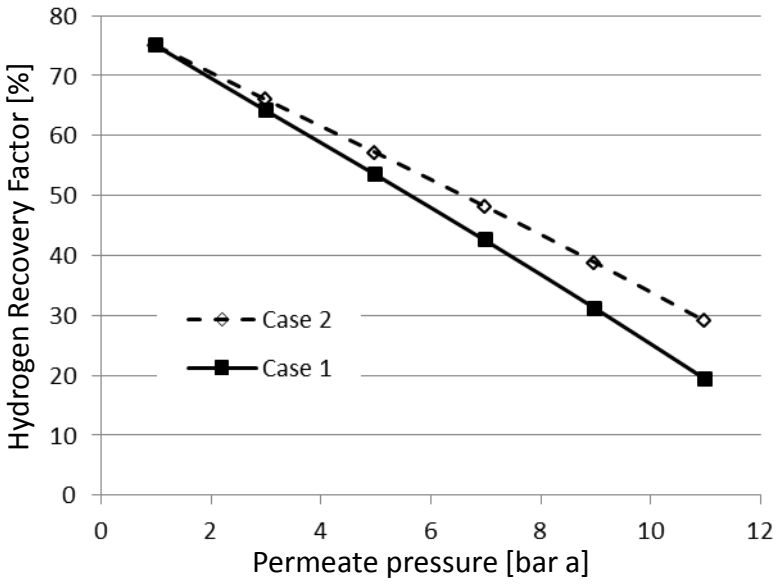

Figure 7. HRF dependency on permeate pressure.

1 column figure

Figure 8

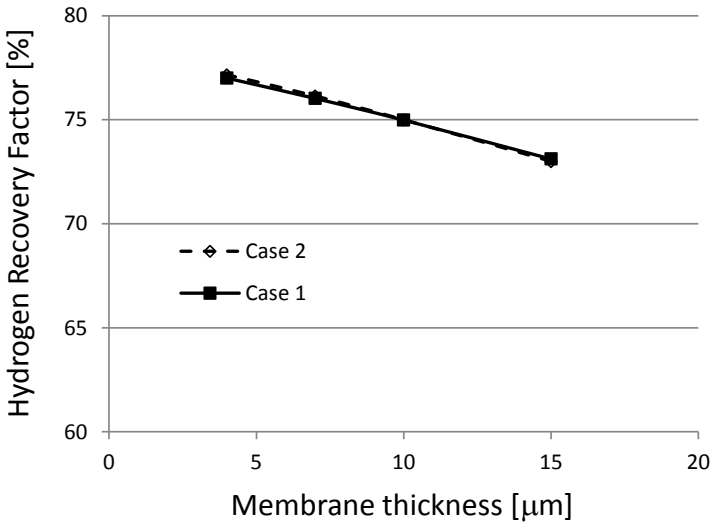

Figure 8. HRF dependency on membrane thickness.

1 column figure

Table 1

Table 1. H_2 membrane separation data.

Case 1 Membrane length L_T	m	11.39
Case 2 Membrane length L_T		10.76
Case 3 Membrane length L_T		10.03
Diameter of feed gas surrounding one membrane tube in model d_1	m	$6.0 * 10^{-2}$
Outer diameter of porous support d_2	m	$3.0*10^{-2}$
Inner diameter of porous support d_3	m	$2.60*10^{-2}$
Membrane area	m^2/membrane	1.36
Sieverts' exponent, n	---	0.5
Feed side pressure	bar a	41
Membrane thickness	m	$10.0*10^{-6}$
Support porosity/tortuosity	---	0.35
Support layer pore diameter	m	$3.4*10^{-6}$
Membrane permeability	$kmol*m/m^2*s*Pa^{0.5}$	$2.0*10^{-11}$
Activation energy, Sieverts law	J/kmol	$1.28*10^{-4}$
Molar flow per membrane	kmol/s	$1*10^{-3}$
Operating temperature	°C	400

Table 2

Table 2. Case 1 (HTS only) stream flow rates and compositions [mole fractions] before and after separation processes. Stream numbers refer to Figure 3.

Stream #	1	2	3	4	5
	Shifted syngas	Shifted, H_2-depleted syngas	Shifted, dried, H_2-depleted syngas	Captured CO_2	Volatiles from CO_2 separation (GT fuel)
kmoles/s	7.833	5.822	3.112	1.684	1.428
H_2	0.3425	0.1152	0.2155	0.0002	0.4692
CO	0.0300	0.0404	0.0755	0.0020	0.1622
H_2O	0.3459	0.4655	0.0000	0.0000	0.0000
CO_2	0.2375	0.3196	0.5980	0.9944	0.1307
CH_4	0.0001	0.0001	0.0002	0.0000	0.0004
N_2	0.0382	0.0514	0.0962	0.0021	0.2073
Ar	0.0058	0.0078	0.0146	0.0014	0.0302

Table 3

Table 3. Case 2 (HTS and LTS, membrane feed pressure 41 bar) stream flow rates and compositions [mole fractions] before and after separation processes. Stream numbers refer to Figure 3.

Stream#	1	2	3	4	5
	Shifted syngas	Shifted, H_2-depleted syngas	Shifted, dried, H_2-depleted syngas	Captured CO_2	Volatiles from CO_2 separation (GT fuel)
kmole/s	7.159	5.012	3.157	1.890	1.267
H_2	0.3999	0.1428	0.2267	0.0002	0.5646
CO	0.0077	0.0110	0.0174	0.0005	0.0428
H_2O	0.2591	0.3701	0.0000	0.0000	0.0000
CO_2	0.2850	0.4072	0.6463	0.9955	0.1254
CH_4	0.0001	0.0002	0.0003	0.0000	0.0007
N_2	0.0418	0.0598	0.0949	0.0023	0.2331
Ar	0.0063	0.0090	0.0143	0.0015	0.0334

Table 4

Table 4. Results from heat and mass balance study, hydrogen produced at 400°C and 1 bar a.

		Case 1	Case 2	Case 3
Coal flow rate	t/h	136.46	136.46	136.46
Coal LHV	MJ/kg	25.17	25.17	25.17
Thermal energy of fuel	**MW_{th}**	**954**	**954**	**954**
Thermal energy for coal drying	**MW_{th}**	**8**	**8**	**8**
H_2 product	kg/s	4.1	4.3	4.3
LHV H_2	MJ/kg	119.96	119.96	119.96
Thermal energy of H_2 product	**MW_{th}**	**487**	**519**	**519**
H_2 production thermal efficiency	**%**	**50.6**	**54.0**	**54.0**
Gas turbine output	MW_e	87.3	73.3	73.3
Steam turbine output	MW_e	85.9	82.8	82.7
Gross power output	MW_e	**173.2**	**156.1**	**156.0**
ASU power consumption	MW_e	12.13	12.13	12.13
O_2 compression	MW_e	11.61	11.61	11.61
N_2 to gasifier compression	MW_e	5.11	5.11	5.11
Selexol H_2S removal	MW_e	0.4	0.4	0.4
Syngas Compressor	MW_e	-	-	4.3
CO_2 capture	MW_e	14.15	15.69	12.1
Power Island aux.	MW_e	3.083	2.4	2.4
Coal Handling	MW_e	1.4	1.4	1.4
Other	MW_e	0.6	0.6	0.6
Total ancillary power consumption	MW_e	**48.5**	**49.3**	**50.0**
Net power output	MW_e	**124.7**	**106.8**	**106.0**
Electric efficiency	**%**	**18.2**	**16.4**	**16.2**
Overall first law efficiency	**%**	**63.5**	**65.1**	**65.0**
CO_2 captured	kg/s	73.7	82.8	82.8
CO_2 emitted	kg/s	18.6	9.5	9.5
CO_2 capture ratio	**%**	**79.9**	**89.7**	**89.7**
Membrane area	**m^2**	**8409**	**7260**	**6767**

Table 5

Table 5. Power consumption and surplus/deficit when including H2 liquefaction in Cases 1 and 2.

			H2 liquefaction power consumption (MW_e)		Power deficit/surplus (MW_e)	
			Case 1	Case 2	Case 1	Case 2
Current liquefaction technology	13,7	kWh_e*	200,0	213,5	-75,3	-106,7
Future liquefaction technology	8,1	kWh_e*	118,3	126,2	6,4	-19,5

*including H2 compression from 1 bar and 30°C